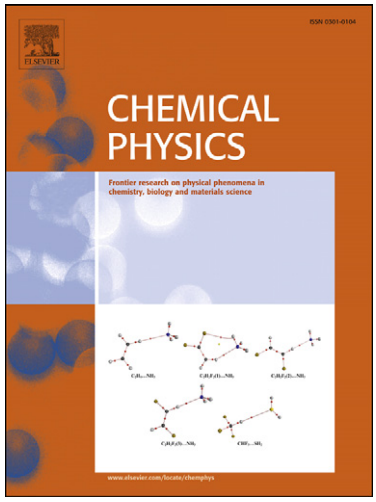

Spectroscopic characterization and aggregation of azine compounds in different media

María Noel Urrutia, Cristina Susana Ortiz

PII: S0301-0104(12)00455-7
DOI: http://dx.doi.org/10.1016/j.chemphys.2012.12.005
Reference: CHEMPH 8708

To appear in: *Chemical Physics*

Received Date: 5 September 2012
Accepted Date: 4 December 2012

Please cite this article as: M.N. Urrutia, C.S. Ortiz, Spectroscopic characterization and aggregation of azine compounds in different media, *Chemical Physics* (2012), doi: http://dx.doi.org/10.1016/j.chemphys.2012.12.005

Spectroscopic characterization and aggregation of azine compounds in different media.

María Noel Urrutia and Cristina Susana Ortiz*

Departamento de Farmacia, Facultad de Ciencias Químicas, Universidad Nacional de Córdoba, Ciudad Universitaria, X5000HUA, Córdoba, Argentina.

*Corresponding author. Tel.: +54-351-5353865 int. 53356; FAX: +54-351-5353865 int. 53364.
Departamento de Farmacia, Facultad de Ciencias Químicas, Universidad Nacional de Córdoba. Haya de La Torre esq. Medina Allende, Ciudad Universitaria, X5000HUA, Córdoba, Argentina.
E-mail address: crisar@fcq.unc.edu.ar (C. S. Ortiz).

Abstract

In this study, we have reported for the first time a complete experimental investigation on the compound Neutral Red and the new monobrominated derivative in different media as a function of the concentration. These compounds belong to the quinone-imine class of dyes and have good potential to be applied as photosensitizers in Photodynamic Therapy.

Although the aggregation of Neutral Red has been reported by several authors, this has not been thoroughly evaluated due to spectral changes occurring depending on the solvent and concentration of dye.

We investigated and compared the effects of aggregation properties in water, ethanol, water-ethanol mixtures, water-polyethylene glycol 400 (75:25 v/v) and N,N-dimethylformamide.

An analysis of the changes in the absorption spectra with respect to the solvent as a function of dye concentration together with theoretical calculations confirmed the monomeric species and the formation of different types of aggregates in this class of compounds.

Keywords

Neutral Red

Synthesis

Bromination

Aggregation

UV-Vis spectroscopy

1. Introduction

The use of dyes in the biomedical area has seen a remarkable growth in research interest in recent years and is probably the most rapidly expanding area of dye chemistry at the present time. The potential biomedical applications of dyes include the general areas of bioanalysis, medical diagnostics and the therapeutic treatment of disease. There are several other applications that might be considered within biomedicine, such as histology, fluorescent biolabelling and fluorescent bioprobes [1].

Photodynamic therapy (PDT) is a therapeutic modality not only applicable for the treatment of superficially localized tumors, but is also associated with the antiviral and bactericidal properties of dyes [2-4]. PDT can be defined as the systemical, local or topical administration of a nontoxic drug or dye known as photosensitizer (PS), which acquires the desired activity only when it is excited by light of an appropriate wavelength. The excitation of PS results in the production of sufficient reactive oxygen species (ROS) to produce a cytotoxic effect [5,6].

Neutral Red (NR) is a phenazine based dye very useful as a biological probe and has been widely utilized for various purposes in many biological systems, among which is the staining of cellular particles and the intracellular pH indicator. In addition, NR has been used as a PS in PDT and good results have been obtained [7,8].

It is well known that the ionic dyes tend to aggregate in diluted solutions, leading to dimer formation, and sometimes to even higher order aggregates. In such cases the molecular nature of the dyes is strongly affected by ionic strength, temperature, presence of organic solvents, dye concentration and structure. Aggregation may rise with an increase of dye concentration or ionic strength, but will decrease with rising temperature or the addition of organic solvents [9,10].

It has been reported that the formation of aggregate in solution produces significant changes in the absorption and emission spectra [11], thus impairing the photochemical response [12] and reducing the lifetimes of the excited state, most probably as a result of enhanced radiationless excited state dissipation

and lowering of the quantum yields of the excited states and of the $^1O_2$ generation [13].

On the other hand, one strategy to increase the efficiency of a spin-forbidden electronic transition from a singlet to a triplet state (intersystem crossing) and regulate the quantity of $^1O_2$ generation is the introduction of heavy atoms into a molecule [14].

Based on the above-mentioned research, we addressed the synthesis of new phenazine cationic dyes. As the chemical structure of NR permits the addition of substituents by aromatic electrophilic substitution using halogens [15], we synthesized Neutral Red monobrominated (NRBr) and Neutral Red monoiodinated (NRI), with their molecular structures being shown in **Scheme 1**. In addition, we have examined the influence of dye concentration and different solvents on the aggregate formation, since the formation of aggregates modifies the photophysical and photochemical properties of a dye, and therefore affects its ability to act as a PS [16,17]. We have chosen for this study different media such as ethanol and polyethylene glycol (PEG) 400 because they are FDA approved cosolvents for the parenteral dosage form [18,19]. Also, we investigated phenazine dyes in *N,N*-dimethylformamide (DMF) as it is known to be a good monomerizing solvent [20]. Absorption UV–Vis spectroscopy was used because it is one of the most suitable methods for quantitatively studying the aggregation properties of dyes as a function of concentration [9,21].

Finally, the experimental data were compared with theoretical calculations and we confirmed the monomeric species of the dyes.

2. Experimental Methods

2.1. Materials /Chemicals

Neutral red hydrochloride (3-amino-7-dimethylamino-2-methyl phenazine hydrocholoride) was purchased from Sigma Chemical Co. (St. Louis, MO) (Fluka Chemicals) and used as received. We confirmed by reversed-phase high-performance liquid chromatography (RP-HPLC) analysis that its purity was > 98 %. All the solvents used were of pro-analysis and HPLC grade (Cicarelli, Sintorgan, Anedra). All chemicals were obtained commercially and were of the

highest purity form. Solutions of bromo were prepared with molecular bromo (Carlo Erba) with a purity > 99.9%.

Aqueous solutions were prepared using ultrapure water from the Milli-Q® water purification system (Millipore Corporation, USA). Deuterodimethylsulfoxide (DMSO-d_6) was purchased from Sigma Chemical Co. (St. Louis, MO) and had a purity > 99.8%.

TLC were carried out using on 250 µm silica gel plates (E. Merck) with chloroform: methanol (92.5: 7.5 v:v) as the solvent system and were visualized with UV light at λ=254 nm.

2.2. Instrumentation

Absorption spectra were carried out at room temperature with an Evolution 300 spectrophotometer using 1 cm path length quartz cells. Spectral curves were recorded in aqueous solution, ethanol, water:ethanol mixtures, DMF and water:PEG 400 mixture, from 10^{-7} M to 10^{-3} M between 200 and 700 nm. All experiments were carried out at least twice with consistent results. Stock solutions of dyes were prepared in duplicate and then diluted appropriately with the same solvent.

NMR spectra were recorded on an RMN Bruker AVANCE II 400 Nuclear Instrument using DMSO-d_6 where the solvent and δ values are given in ppm.

Mass spectra were determined in solid state on a Cuadrupolar Finnigan 3300 F-100 mass spectrophotometer by electron ionization (EI-MS) at 70 eV. Electrospray ionization mass spectra (ESI-MS) were recorded on a Varian 1200L triple-quadrupole LC–MS spectrometer. ESI high-resolution mass spectra (HSMS) were recorded on a Bruker Micro QTOF II spectrometer equipped with an ESI source. Samples were introduced dissolved in methanol HPLC grade at a final concentration of 10 µg/ml.

FT-IR spectra were recorded in the range of 4000-600 cm^{-1} on a Nicolet 5SXC FT-IR spectrometer as KBr pellets.

RP-HPLC was carried out using an Agilent 1100 Series HPLC system (Agilent Technologies, Waldbronn, Germany) equipped with an autosampler, a column thermostat and a UV-Vis detector set at 280 nm and 540 nm. A reversed-phase C18 (Supelco®) column (4.6 mm x 250 mm, 5µm) with guard column and flow rate of 1.0 ml/min were used. The mobile-phase was prepared with methanol

HPLC grade and an aqueous solution of trimethylammonium phosphate 83 mM (70:30 v/v) using Milli-Q® water, and the pH of the mobile-phase was 4.76.

2.3. Computational Details

Theoretical calculations were performed with the GAUSSIAN 03 suite of programs. All geometry optimizations were computed using the hybrid density functional B3LYP and the standard 6-31+G(d) basis set. The stationary points were located with the Berny algorithm using redundant internal coordinates. Analytical Hessians were computed to determine the nature of stationary points (one and zero imaginary frequencies for transition states and minima, respectively) and to calculate the unscaled zero-point energies (ZPEs) as well as the thermal corrections and entropy effects using the standard statistical-mechanics relationships for an ideal gas. Nonspecific solvent effects were described by using the self-consistent reaction field (SCRF) approach in Tomasi's formalism. Single point PCM [B3LYP/6-31+G(d)] calculations were performed to estimate the UV-spectrum profile of the dyes.

2.4. Synthesis: General Aspects

All the solutions were freshly prepared before being used. The reaction progress and purity of the compounds were monitored by RP-HPLC and TLC. The reaction solvent was removed under reduced pressure and the solid residue was analyzed by RP-HPLC. During all the experiments, the reaction mixture was stirred and the round-bottom flask was protected from the light.

2.5. Characterization

Neutral Red (NR): IR (KBr, cm^{-1}): υ 1622, 1525, 1495 (C=C) 1194, 1009 (C-N) 880, 804 (oop C-H). t_R RP-HPLC (n=7, min.): 4.72±0.07. R_f TLC (n=7): 0.20±0.05. ^{1}H-RMN (DMSO-d_6, 400 MHz): δ (ppm)= 2.320 (s,3H), 3.219 (s, 6H), 6.764 (d,1H, J_{meta}=2.4807), 6.894 (s,1H), 7.465 (dd,1H, J_{orto}=9.689, J_{meta}=2.481), 7.735 (s,1H), 7.867 (d,1H, J_{orto}=9.689). ^{13}C-RMN (DMSO-d_6, 400 MHz): δ (ppm)= 18.181, 40.373, 92.338, 93.047, 118.979, 130.961, 131.183, 131.750, 133.941, 134.192, 135.283, 137.005, 154.127, 156.633. EI-MS (70 eV, m/z): 252 $[M]^+$, 209, 181. ESI-MS (m/z): 253.1 $[MH]^+$, MS-MS (m/z): 237.0, 210.0. HRMS (ESI): Calcd for $C_{15}H_{17}N_4$ $[MH]^+$: 253.3224, found: 253.1466.

Neutral Red monobrominated (NRBr): In order to prepare NRBr, 10.0 mg ($3.46x10^{-2}$ mmol) of commercial dye NR were dissolved in 10 ml of glacial acetic acid and then a solution of bromine in glacial acetic acid ($3.46x10^{-2}$ mmol, 5 ml) was added dropwise with constant stirring. The reaction solvent was removed under reduced pressure at 55-60ºC, and 10 ml of ethanol was added to dissolve the reaction product which was then filtered. The ethanolic media was removed at 40ºC and the crude product did not need any further purification. The best reaction conditions were radio dye:bromine 1:1 at room temperature for 30 minutes (purity > 98 % by RP-HPLC).
IR (KBr, cm^{-1}): υ 1611, 1532, 1496 (C=C) 1197, 1020 (C-N) 878, 802 (oop C-H) 679 (C-Br). t_R RP-HPLC (n=7, min.): 6.43±0.08. R_f TLC (n=7): 0.70±0.06. ^{1}H-RMN (DMSO-d_6, 400 MHz): δ (ppm)= 2.416 (s,3H), 3.247 (s,6H), 7.218 (s,1H), 7.539 (d,1H, J_{orto}=9.612), 7.740 (s,1H), 7.864 (d,1H, J_{orto}=9.612). ^{13}C-RMN (DMSO-d_6, 400 MHz): δ (ppm)= 19.244, 43.468, 94.870, 97.981, 120.250, 123.025, 129.697, 130.557, 131.564, 135.736, 136.504, 148.400, 152.438, 154.442. EI-MS (70 eV, m/z): 330 $[M]^+$, 332 $[M+2]^+$, 287, 250, 235, 207. ESI-MS (m/z): 331.0 $[MH]^+$, 332.9 $[MH+2]^+$, MS-MS (m/z): 251.0. HRMS (ESI): Calcd for $C_{15}H_{16}BrN_4$ $[MH]^+$: 331.0553, $[MH+2]^+$: 333.0533; found: 331.0564, 333.0547.

Neutral Red monoiodinated (NRI): This compound was synthesized by a modified method reported in the literature [22]. All the solutions were prepared in glacial acetic acid:water solution (9:1, v/v). In order to prepare NRI, 3.0 mg ($1.04x10^{-2}$ mmol) of commercial dye NR were dissolved in a round-bottom flask. Solutions of sodium periodate (2.2 mg; $1.04x10^{-2}$ mmol) and sodium chloride (1.2 mg; $2.08x10^{-2}$ mmol) were added with constant stirring to the NR solution, followed by potassium iodine solution (1.7 mg; $1.04x10^{-2}$ mmol).
The solvent was removed under reduced pressure at 60ºC and then dichloromethane was added to the round-bottom flask to dissolve the iodinated product which was then filtered. This solvent was removed at 35ºC. The best reaction conditions were radio dye:sodium periodate:potassium iodine:sodium chloride 1:1:1:2 at 25 ºC for 6 hours. As the potassium iodine was very unstable in acid and quickly decomposed to a strong yellow solution, the solution was freshly prepared.

Although its EI-MS spectra confirmed a peak 380 $[MH]^+$, we attributed this to a molecular ion of NRI, that was unstable in the solid state, under N_2 atmosphere, to 4°C and dark ambient, in contrast to its analog NRBr. Therefore, we decided not to study it due to this compound not being an efficient PS.

3. Results and discussion

Absorption spectra of NR at different concentrations in aqueous solutions were analyzed on the basis of the shift of maximum absorption wavelength (λ_{max}) and are shown in **Figure 1**. It is interesting to note a relatively significant blue shift of 13 nm when the dye concentration was increased ($6.92x10^{-7}$ M - $6.92x10^{-5}$ M). **Figure 1, inset,** shows twelve representative normalized absorption spectra in aqueous solutions. The presence of aggregates was revealed by the appearance of an isobestic point at 575 nm.

According to the Exciton theory, a monomer-dimer model is not sufficient to explain the above results and it was therefore necessary to invoke the formation of higher aggregates. The experimentally observed spectral shift in water as a function of concentration resulted in an aggregate band hypsochromic, with the aggregate being formed by the association of dye molecules in which the molecules were arranged one above the other [11,23]. Similar results have been reported by other authors for Thionine, a thiazine dye [24]. Since the spectral changes upon aggregation are dependent in many ways on the properties of the isolated molecule, the degree of spectral changes is not a direct indication of the degree of aggregation [25].

Similar studies of NR were carried out in water:ethanol mixtures (95:5 v/v and 90:10 v/v), which demonstrated that the organic solvent prevented the formation of aggregates [9,26] since the blue shifts were 10 nm and 3 nm, respectively (data not shown). We attribute these results to specific interactions between the solute and the solvent molecules, since the aggregation of the dye in solution depends strongly on the solvent nature [27].

The change of absorbance of NRBr in aqueous solutions for an increase in concentration is shown in **Figure 2**. The dye exhibited one absorption band at 535 nm with a weak shoulder at 468 nm. The absorption band and the shoulder

appeared even at very low concentrations (<2.71x10^{-6} M) and increased as a function of dye concentration in the solution. We assigned the absorption maximum at 535 nm to the aggregate form and absorption band at 468 nm to the monomeric species, since by increasing the concentration the aggregate predominated over the monomeric form **(Figure 2, inset)**. This was clear due to the absorbance increases being more significant at 535 nm than at 468 nm and these observations were corroborated when comparing with the results shown in **Figure 3**. This study was carried out in water:ethanol mixture 75:25 v/v, at different concentrations of the compound NRBr. Furthermore, absorption spectra of highly concentrated NRBr revealed evidence of two absorption bands with maxima at 540 nm and 458 nm. On the basis of the data in **Figure 3 inset**, the monomeric form of NRBr was responsible for the 458 nm band, whereas the 540 nm band did not follow the Lambert-Beer Law and may have been attributed to NRBr aggregates. As for NR, these results for NRBr confirm that the organic solvent favored the disruption of the aggregates [16,26].

The assignation of both absorption bands (the aggregate and monomer of NRBr) in highly concentrated solutions of dye in pure water (**Figure 2**) and water:ethanol mixture, 75:25 v/v, (**Figure 3**), was confirmed by the absorption bands in pure ethanol at the different concentrations shown in **Figure 4 and Figure 4, inset**. In this solvent, at low dye concentrations, the absorption peak at 455 nm was due to the monomeric species, but as the concentration of NRBr increased, a second peak at a higher wavelength appeared. This new peak at 545 nm became greater when the dye concentration was higher than 3.25x10^{-5} M. This dye existed only as a monomer in ethanol at lower concentrations than 1.62x10^{-5} M, with the changes in the absorption spectra with dye concentration being more pronounced in this solvent than those observed in pure aqueous solution (**Figure 2**). In **Figure 4**, the curves **a-d** can be attributed to the monomer of dye (yellow solutions), curves **e-f** as a mixture of monomer and aggregate (orange solutions) and curves **g-l** as a mixture of monomer and aggregate where the aggregate predominated (red solutions). Over the concentration range studied, the Lambert-Beer Law was not obeyed and the appearance of a new band was rationalized in terms of dye aggregation [10,28]. The concentration dependence of NRBr in ethanol resulted in an aggregate band bathochromic (J-band), so the spectra of the aggregate were red-shifted

with respect to the monomeric form. These kind of aggregates, are called J-aggregates [11,23].

Absorption spectra of NR in pure ethanol, recorded as a function of dye concentration, are shown in **Figure 5**. The analyses of the results suggest that if the concentration of NR is small enough (<1.04x10^{-5} M), the aggregate will not be present in the solution. Increasing dye concentration led to an increase of the intensity of monomer band at 464 nm and the formation of an aggregate at 537 nm. The development of the second peak (aggregate form) at concentrations above 1.39x10^{-5} M and at a higher wavelength, suggests head-to-tail aggregates (J-band) **(Figure 5 inset)** [11,23]. The concentration dependencies of NR spectra in ethanol were qualitatively similar to compound NRBr (**Figure 4**), due to both dyes in dilute solutions showing a maximum near 460 nm and changes in their spectral curves with the aggregation causing alterations and forming new easily resolved absorption bands. The NRBr aggregate formation in ethanol was observed at slightly higher concentrations (>1.63x10^{-5} M) in comparison with NR (>1.04x10^{-5} M), which indicates that in this solvent there were no significant differences as a consequence of the presence of a bromine atom. These observations differ from the analysis of some other authors [29], who affirmed that the tetrabromoderivative (eosin Y) had a greater tendency to aggregate than its precursor (fluorescein), and consequently halogenations were found, which were able to promote the aggregation of xanthene dyes.

In the studies concerning the analyses of the NR and NRBr dyes in various proportions of water:ethanol, the concentrations chosen were 6.93x10^{-6} M and 2.71x10^{-5} M for NR and NRBr respectively due to the aggregates in pure ethanol were not detectable.

As evident from **Figure 6 A**, the shapes of the absorption spectra of NR in water:ethanol mixtures, 75:25 v/v (curve **d**) and 50:50 v/v (curve **e**), were different from those in water:ethanol mixture 25:75 v/v (curve **f**) and pure ethanol (curve **g**), with NR absorption depending on the solvent. The addition of increasing amounts of ethanol to pure water, gradually decreased the absorption maximum band at 537 nm in pure water (aggregate) and increased the absorption band at 464 nm in pure ethanol (monomer). This revealed that the aggregate was not detectable in water:ethanol 25:75 v/v or pure ethanol.

This can be explained bearing in mind that the strength of the aggregation between two or more dye molecules depends on the structure of the dye, the solvent and the presence or absence of electrolytes. In general, dyes aggregate more strongly in water than in organic solvents [16,21,30].

The absorption spectra of NRBr in different water:ethanol mixtures, are shown in **Figure 6 B**. In pure water (curve **a**) and in a water-ethanol mixture 95:5 v/v (curve **b**), the dye exhibited an absorption band at 538 nm (aggregate) and a shoulder at 468 nm (monomer). However, at higher ethanol proportions, only the band of monomer appeared, centered at around 458 nm. Therefore, these results suggest that the higher ethanol proportions resulted in the decrease in absorbance at 538 nm with an increased definition in the monomer band. It can also be seen from this Figure that decreasing dielectric constant values (increase of ethanol) favored the dye monomeric species, and this might have been due to solvent-solvent interactions and/or a specific interaction between the solvent and hydrogen atom from NH_2 group in the dye molecule [28,31].This reveals that practically no aggregate was formed in pure ethanol, water-ethanol mixtures 25:75 v/v or 50:50 v/v.

An interesting comparison arises from the absorption spectra of both dyes in the water-ethanol mixture 50:50 v/v (**Figure 6 A** curve **e** and **Figure 6 B** curve **e**), where we demonstrated that for compound NR the aggregate form was evident at 537 nm whereas for dye NRBr alone the monomeric form was observed at 458 nm.

NR and NRBr were studied in different solvents which increase the quantity of monomers in solutions such as DMF [20,32] and PEG 400 [19,33] both known to be good monomerizing solvents, to continue the studies of the monomer form of dyes and to attempt to corroborate the assignation of the different bands. Therefore, considering that aggregate formation is inhibited in organic solvents, and even more so in PEG 400, the behavior of NRBr in water:PEG 400 mixture 75:25 v/v as function of dye concentration was analyzed (**Figure 7**). In this mixture, the monomer of the dye was the predominant species and was responsible for the principal band at 450 nm. A very weak shoulder was observed around 530 nm, which was assigned to the aggregated form of NRBr. An interesting observation was that the shape of the absorption spectra was not modified in the concentration range studied (5.42×10^{-6} - 8.14×10^{-5} M).

Furthermore, on analysis of the normalized absorption spectra (**Figure 7, inset**) all the spectral curves at 450 nm were found to be overlaid and obeyed the Lambert-Beer law.

These results clearly confirm our assignment in water:ethanol mixture 75:25 v/v (**Figure 3**). Then, when the effects of both cosolvents, ethanol and PEG 400 were compared at the same proportion mixtures with water, it was clear that PEG 400 favored more the monomeric species of the compound, in agreement with the literature [19,33] therefore, this solvent is more relevant for different biological environments.

An analysis was also performed for NR in the same mixture of solvents (**Figure 8**). In this case, we observed a band of an aggregate form of the dye, with a maximum absorption wavelength of around 542 nm. This species was predominant at all the concentration range studied ($3.46x10^{-6}$ M – $4.85x10^{-5}$ M), and the shoulder at 475 nm assigned to the monomer species was evident and strong in all spectral curves. The normalized absorption spectra at 542 nm (**Figure 8, inset**) presented the same tendency observed for the new dye NRBr, with the spectral curves being almost overlaid.

When we compared the absorption spectra of NR and NRBr in water:PEG 400 75:25 v/v, it was clear that the aggregate of the new dye in solution was detectable at higher concentrations than NR. Based on this observation, we suggest that substitution with heavy atoms, such as bromine, did not favor the formation of aggregates and may have improved the photochemical properties of this dye and their potential use as PS in the PDT applications [14,15].

Absorption data in DMF for increasing NR concentrations are shown in **Figure 9 A**. Raising the dye concentration in solution increased the absorbance of the monomeric form (450 nm), and at higher concentrations a new band appeared assigned to the NR aggregate (540 nm) which became the maximum of the spectral curve at greater concentrations (**Figure 9 A, inset**).

These results are clearly similar with those obtained in pure ethanol (**Figure 5**). However, it is evident that the aggregate of NR appeared at a higher concentration in DMF ($3.46x10^{-5}$ M) than in ethanol ($1.39x10^{-5}$ M), this can be explained, according to the literature, due to DMF being a solvent which favors the monomeric species [20,32].

The new dye, NRBr **(Figure 9 B)** showed an absorption band at 450 nm assigned to the monomeric species in pure DMF. At the highest dye concentration studied ($2.71x10^{-4}$ M), a weak shoulder appeared at around 555 nm assigned to the aggregated form, but the monomeric form was still the predominant band in the spectrum (the maximum of the spectral curve). The normalized spectral curves of NRBr in DMF **(Figure 9 B, inset)** revealed that the monomeric band at the different evaluated concentrations was overlaid.

If we compare the NRBr absorption spectra in ethanol **(Figure 4)** with the absorption spectra in DMF **(Figure 9 B)** depending on the dye concentration, the same tendency was observed for the NR dye and the band of NRBr aggregate appeared at a higher concentration in DMF ($2.71x10^{-4}$ M), than in ethanol ($2.44x10^{-5}$ M) and this suggests that the solvent plays an important role in aggregation since the spectra showed marked differences in both solvents. As mentioned above, in ethanol there were no significant differences in the aggregation behavior of NR and NRBr. However, in DMF there was a contrast between the absorption spectra of the dyes, and it is clear that in this solvent and PEG 400 the monobrominated derivative was less aggregated, which is an important property of PDT [12,34,35].

Great differences in the aggregation between NR and NRBr were found in DMF and PEG 400, and one of the possible explanations is that the bromine atom increased the lipophilic character of the molecule and prevented the molecular aggregation due to it being a bulky substituent. Therefore, the steric hindrance may have inhibited aggregation among the dye units and resulted in a weak aggregation. Previously, it has been reported that aggregation of some PS in organic solutions can be suppressed by peripheral substitution with long alkyl chains or bulky substituents [36]. Several authors have also confirmed that bulky lipophilic substituents ensure good monomerization, with the *tert*-butyl group having previously been found to inhibit dimerization is more than long alkyl chains [37,38].

It can be concluded that the introduction of a bulky substituent not only enhanced the lipophilic character of NR, but also prevented its molecular aggregation in solution due to a steric reason, potentially resulting in superior photochemical and photophysical characteristics, which enhanced the PDT properties [39,40]. Nevertheless, these observations contradict the predictions

of some authors who argue that increasing the lipophilicity of compounds, causes a rise in their aggregation tendencies [12,41].

Halogens can modify the electronic properties of the dyes because of the resonance effects, and this has been widely studied in copper and zinc phthalocyanines substituted with electronegative fluorine and chlorine atoms. The differences observed could be a result of changes in the distribution of π-electrons, due to mesomeric and/or inductive effects. In addition, the molecular structure of dyes and their environment can strongly influence the point charge effect, which consequently affects their photophysical properties [42].

The different kinds of interactions between molecules, such as Van der Waals, intermolecular hydrogen bonding and hydrogen bonding with the solvent, could also explain the aggregation behavior. In fact, various mechanisms have been suggested to explain the forces holding dye ions together in solution, and it is necessary to point out that for a given dye/solvent system, more than one mechanism may be important [16]. To form the simplest aggregate the dimer, the dye-dye interaction must be strong enough to overcome any other forces which would favor solvation of the monomer [28].

The lower aggregation of the new derivative NRBr is a very important result due to aggregation shortening the triplet-state lifetimes and reducing the singlet oxygen quantum yield [37]. Also from a biological viewpoint, it was expected that the new compound, compared to the starting reagent, would predominate as monomers (active form) in cell membranes, so this could be a better PS in PDT.

Due to the large amount conflicting results concerning aggregation in the literature, we decided to attempt to confirm the assignments made by theoretical calculations and then compared the experimental UV-vis spectra of NR and NRBr in ethanol (**Figure 10**) and DMF (data not shown) with the calculated spectra.

The maximum absorption was calculated after initial geometry optimization, and the calculations revealed that the general shapes of the curves were indeed similar, with the maxima in the visible spectra being near at the experimental result and assigned to the monomeric form of both the dyes.

Figure 10 shows the simulated excited-state (λ_{ES}) and the experimental visible absorption band (λ_{Exp}) wavelengths of NR **(Figure 10 A)** and NRBr **(Figure 10**

B) in ethanol. It can be observed that the experimental monomeric band and the theoretical band are very close, but are far from the aggregate band of the dyes, corroborating in this way the monomer assignation in these studied systems. Similar variations between experimental and calculated spectra have also been reported for other compounds [43,44].

4. Conclusions

The aggregation of dyes has fundamental consequences in areas as diverse as bioanalysis, medical diagnostics and the therapeutic treatment of disease. Since the formation of aggregates modifies the absorption spectrum and photochemical properties of a dye, it affects the ability to emit at a certain wavelength or to act as a PS. The applications described above are dependent an aggregation phenomena, which in turn depend on the structure of the dye, the solvent or media, the temperature and the presence or absence of electrolytes. The solvents chosen for this study, ethanol and polyethylene glycol, are used as cosolvents in the pharmaceutical area.

Through an analysis of solvent effects on the spectral properties of NR and NRBr solutions, we have demonstrated interesting results and have shown that different solvents, dye concentrations and substitution in the molecule have a great influence on the aggregation behavior.

In this study, we report for the first time, a complete experimental investigation about the compounds NR and NRBr in different pure and mixture solvents as a function of the concentration. We demonstrate that the new bromine derivative formed aggregates at much higher concentrations in comparison with its precursor and this was associated with the bromine substituent.

The new bromine dye exits as a monomer in ethanol at concentrations below 1.63×10^{-5} M, and at concentrations greater than 2.44×10^{-5} M aggregates have been detected. Changes in the absorption spectra of NRBr in ethanol as a function of dye concentration were more pronounced than those observed in aqueous solution, with the association of this dye in ethanol being considerably weaker than it was in water.

In summary, the results obtained in this study confirm that phenazine dyes NR and NRBr form aggregates and that depend significantly on the solvent and dye concentration. We also demonstrated that in mixed solvents of pharmaceutical interest, the shape, maximum absorption wavelengths and the formation of aggregates depend on the chemical nature of the solvent. Finally, this work demonstrates that the phenazine dye NRBr can have a potential use as PS in PDT, due to it being able to present better photochemical properties, lipophilicity and less aggregation with respect to the starting reagent.

Acknowledgments

Financial support of this research by Secretaría de Ciencia y Técnica de la Universidad Nacional de Córdoba (SECYT-UNC) and Fondo para la Investigación Científica y Tecnológica (FONCYT) of Argentina is gratefully acknowledged.

The authors wish to express their sincere thanks to Dr. Rubén H. Manzo for allowing us the use of the Evolution 300 spectrophotometer. The authors also thank Dr. Diego Andrada for theoretical calculations and helpful discussions. We wish to thank Dr. Gloria Bonetto for developing the nuclear magnetic resonance spectrums. We would like to thank Dr. Paul Hobson (native speaker) for revision of the manuscript.

References

[1] J. C. V. Pais de Moura in: H. S. Freeman and A. T. Peters (eds.) Colorants for non-textile applications, Elsevier, Applied Science Publishers Ltd, England, 1st ed., 2000, p. 189.

[2] H. Yin, Y. Li, Y. Zheng, X. Ye, L. Zheng, C. Li, Z. Xue. Lasers Med. Sci., 2011, DOI: 10.1007/s10103-011-1013-z.

[3] A. C. Borges Pereira Costa, V. M. Campos Rasteiro, C. A. Pereira, E. S. H. da Silva Hashimoto, M. Beltrame Jr., J. Campos Junqueira, A. O. Cardoso Jorge. Arch. Oral Biol. 56 (2011) 1299.

[4] J. P. M. L. Rolim, M. A. S. de-Melo, S. F. Guedes, F. B. Albuquerque-Filho, J. R. de Souza, N. A. P. Nogueira, I. C. J. Zanin, L. K. A. Rodrigues, J. Photochem. Photobiol. B. 106 (1) (2012) 40.

[5] F. C. Rossetti, L. B. Lopes, A. R. H. Carollo, J. A. Thomazini, A. C. Tedesco, M. V. Lopes Badra Bentley. J. Control. Release. 155 (2011) 400.

[6] H. L. Lu, W. J. Syu, N. Nishiyama, K. Kataoka, P. S. Lai. J. Control. Release. 155 (2011) 458.

[7] M. K. Singh, H. Pal, A. C. Bhasikuttan, A. V. Sapre, Photochem. Photobiol. 69 (5) (1999) 529.

[8] B. B. Fischer, A. Krieger-Liszkay, R. I. L. Eggen, Plant. Sci. 168 (2005) 747.

[9] L. Antonov, G. Gergov, V. Petrov, M. Kubista, J. Nygren, Talanta. 49 (1999) 99.

[10] A. G. Gilani, M. Moghadam, S. E. Hosseini, M. S. Zakerhamidi, Spectrochim. Acta A. 83 (2011) 100.

[11] O. Valdes-Aguilera, D. C. Neckers, J. Phys. Chem. 92 (1988) 4286.

[12] C. C. Chang, Y. T. Yang, J. C. Yang, H. D. Wu, T. Tsai, Dyes Pigments. 79 (2008) 170.

[13] T. Nyokong, Coordin. Chem. Rev. 251 (2007) 1707.

[14] A. Gorman, J. Killoran, C. O'Shea, T. Kenna, W. M. Gallagher, D. F. O'Shea, J. Am. Chem. Soc. 126 (2004) 10619.

[15] T. Yogo, Y. Urano, Y. Ishitsuka, F. Maniwa, T. Nagano, J. Am. Chem. Soc. 127 (35) (2005) 12162.

[16] O. Valdes-Aguilera, D. C. Neckers, Acc. Chem. Res. 22 (1989) 171.

[17] S. D. Choudhury, A. C. Bhasikuttan, H. Pal, J. Mohanty, Langmuir. 27 (2011) 12312.

[18] J. W. Millard, F. A. Alvarez-Núñez, S. H. Yalkowsky, Int. J. Pharm. 245 (2002) 153.

[19] Kabir-ud-Din, Z. Yaseen, M. S. Sheikh, Colloid. Surface B. 87 (2011) 340.

[20] P. Zimcik, M. Miletin, Z. Musil, K. Kopecky, L. Kubza, D. Brault, J. Photochem. Photobiol. A. 183 (2006) 59.

[21] A. Ghanadzadeh Gilani, M. Moghadama, M. S. Zakerhamidib, Comput. Meth. Prog. Bio. 104 (2011) 175.

[22] E. Lourdusamy, S. Ravi Kant, S. Arumugam, G. Suryavanshi, S. Swaminathan, Tetrahedron Lett. 47 (2006) 4793.

[23] V. Kumar, G. A. Baker, S. Pandey, S. N. Baker and S. Pandey, Langmuir. 27 (2011) 12884.
[24] W. C. Lai, N. S. Dixit, R. A. Mackay, J. Phys. Chem. 88 (1984) 5364.
[25] A. R. Monahan, N. J. Germano, D. F. Blossey, J. Phys. Chem. 76 (9) (1971) 1227.
[26] K. T. Arun, B. Epe and D. Ramaiah, J. Phys. Chem. B. 106 (2002) 11622.
[27] A. Ghanadzadeh Gilani, R. Sariri, K. Bahrpaima, Spectrochim. Acta A. 5 (2001) 155.
[28] A. R. Monahan, D. F. Blossey, J. Phys. Chem. 74 (3) (1970) 4014.
[29] S. De, S. Das, A. Girigoswami, Spectrochim. Acta A. 61 (2005) 1821.
[30] S. J. Isak, E. M. Eyring, J. Phys. Chem. 96 (1992) 1738.
[31] M. A. Rauf, A. A. Soliman, M. Khattab, Chem. Cent. J. 2 (1), art nº 19 (2008).
[32] P. Zimcik, M. Miletin, H. Radilova, V. Novakova, K. Kopecky, J. Svec, E. Rudolf, Photochem. Photobiol. 86 (2010) 168.
[33] P. Dutta, R. Rai, S. Pandey, J. Phys. Chem. B. 115 (2011) 3578.
[34] Y. N. Konan, R. Gurny, E. J. Allémann, Photochem. Photobiol. B. 66 (2002) 89.
[35] D. K. Chatterjee, L. S. Fong, Y. Zhang. Adv. Drug. Deliv. Rev. 60 (2008) 1627.
[36] P. Zimcik, M. Miletin, K. Kopecky, Z. Musil, P. Berka, V. Horakova, H. Kucerova, J. Zbytovska, D. Brault, Photochem. Photobiol. 83 (2007) 1497.
[37] M. Kostka, P. Zimcik, M. Miletin, P. Klemera, K. Kopecky, Z. Musil, J. Photochem. Photobiol. A. 178 (2006) 16.
[38] S. Bayar, H. A. Dinçer and E. Gonca, Dyes Pigments. 80 (2009) 156.
[39] S. Wei, J. Zhou, D. Huang, X. Wang, B. Zhang, J. Shen, Dyes Pigments. 71 (2006) 61.
[40] P. Zimcik, M. Miletin, J. Ponec, M. Kostka, Z. Fiedler, J. Photochem. Photobiol. A. 155 (2003) 127.
[41] D. Bechet, P. Couleaud, C. Frochot, M. V. Viriot, F. Guillemin, M. Barberi-Heyob, Trends Biotechnol. 26 (11) (2008) 612.
[42] D. Wróbel, A. Siejak, P. Siejak, Sol. Energ. Mat. & Sol. C. 94 (2010) 492.
[43] C. Johnson, S. B. Darling and Y. You, Monatsh. Chem. 142 (2011) 45.

[44] S. R. Stoyanov, C. X. Yin, M. R. Gray, J. M. Stryker, S. Gusarov, A. Kovalenko, J. Phys. Chem. B. 114 (2010) 2180.

Scheme 1

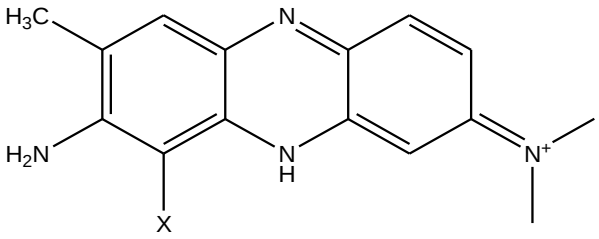

NR X=H
NRBr X=Br
NRI X=I

Scheme Caption 1

Scheme 1: Molecular structure of Azine dyes used in this study.

Figure 1

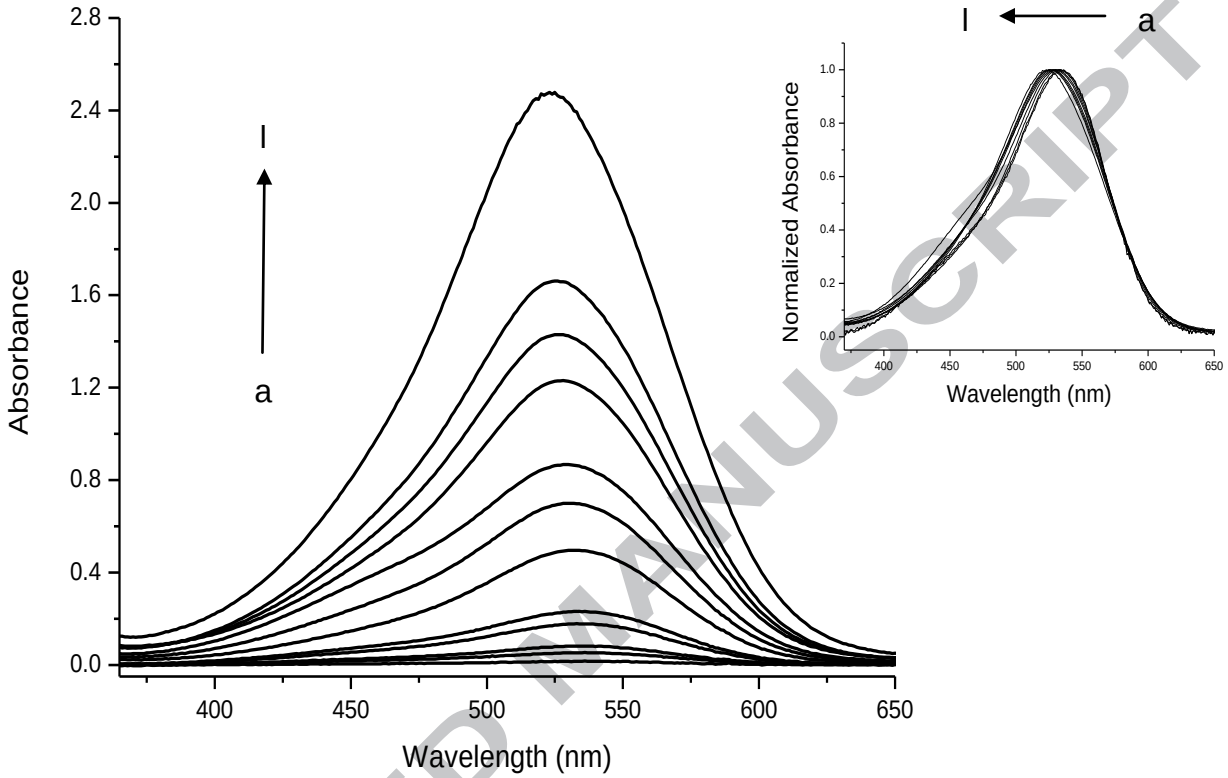

Figure Caption 1

Figure 1: Absorption spectra of **NR** at different concentrations in aqueous solutions. [**NR**] (a) 6.92×10^{-7} M, (l) 6.92×10^{-5} M. Inset: Normalized absorption spectra at 537 nm as a function of concentration.

Figure 2

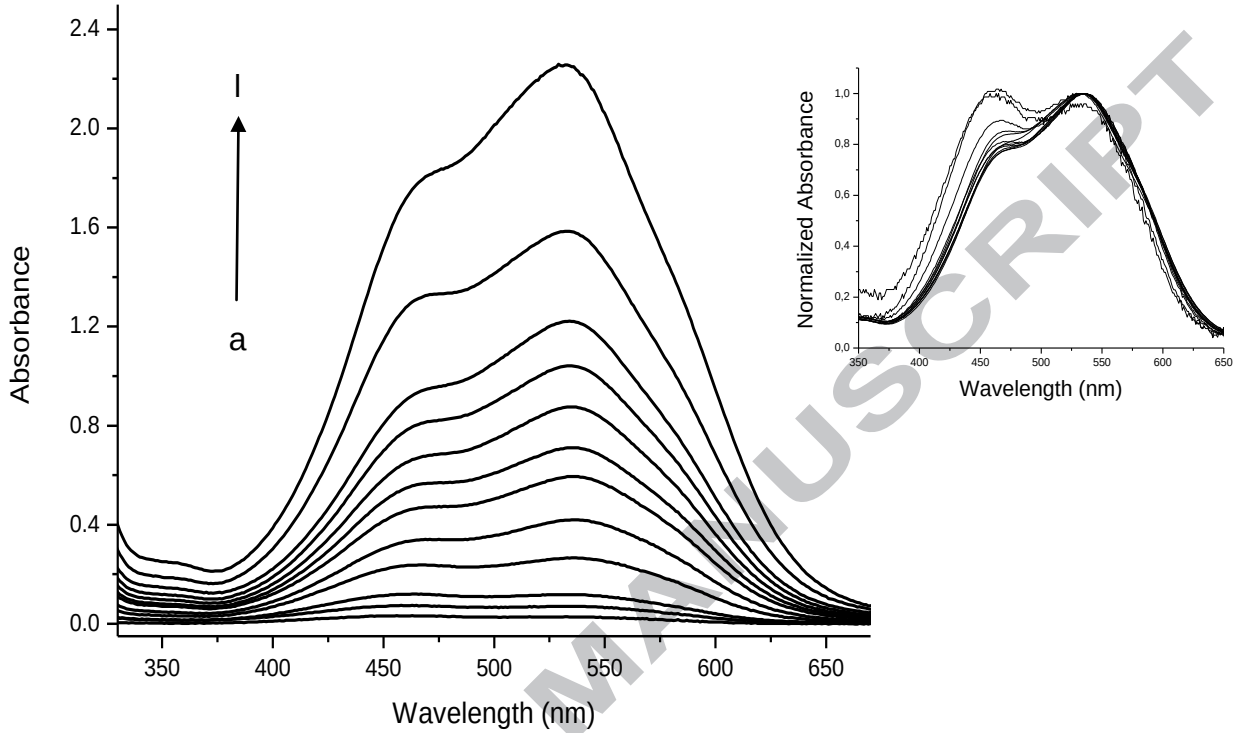

Figure Caption 2

Figure 2: Absorption spectra of **NRBr** at different concentrations in water. [**NRBr**] (a) 2.71×10^{-6} M, (l) 1.36×10^{-4} M. Inset: Normalized absorption spectra at maximum absorption wavelength as a function of concentration.

Figure 3

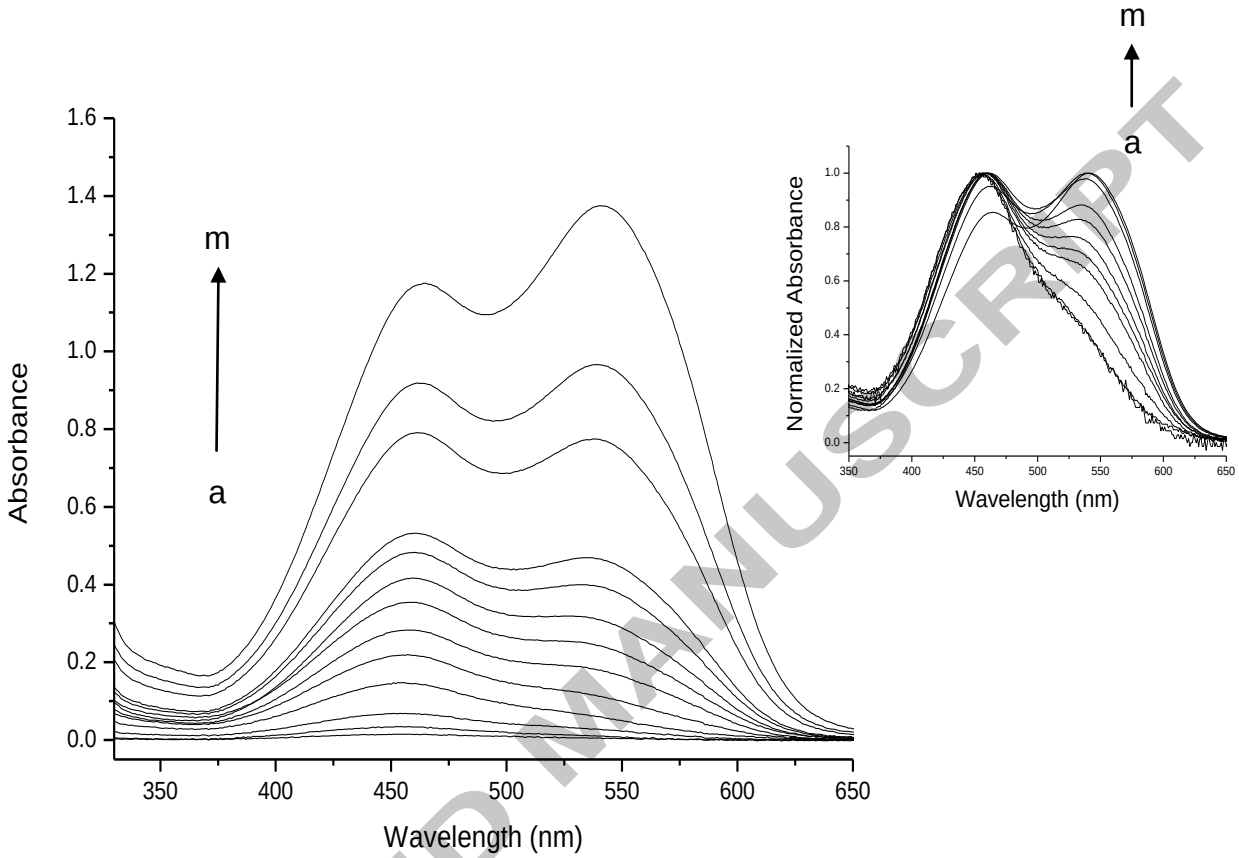

Figure Caption 3

Figure 3: Absorption spectra of **NRBr** at different concentrations in water:ethanol (75:25 v/v). [**NRBr**] (a) 1.08×10^{-6} M, (m) 9.76×10^{-5} M. Inset: Normalized absorption spectra at maximum absorption wavelength as a function of concentration.

Figure 4

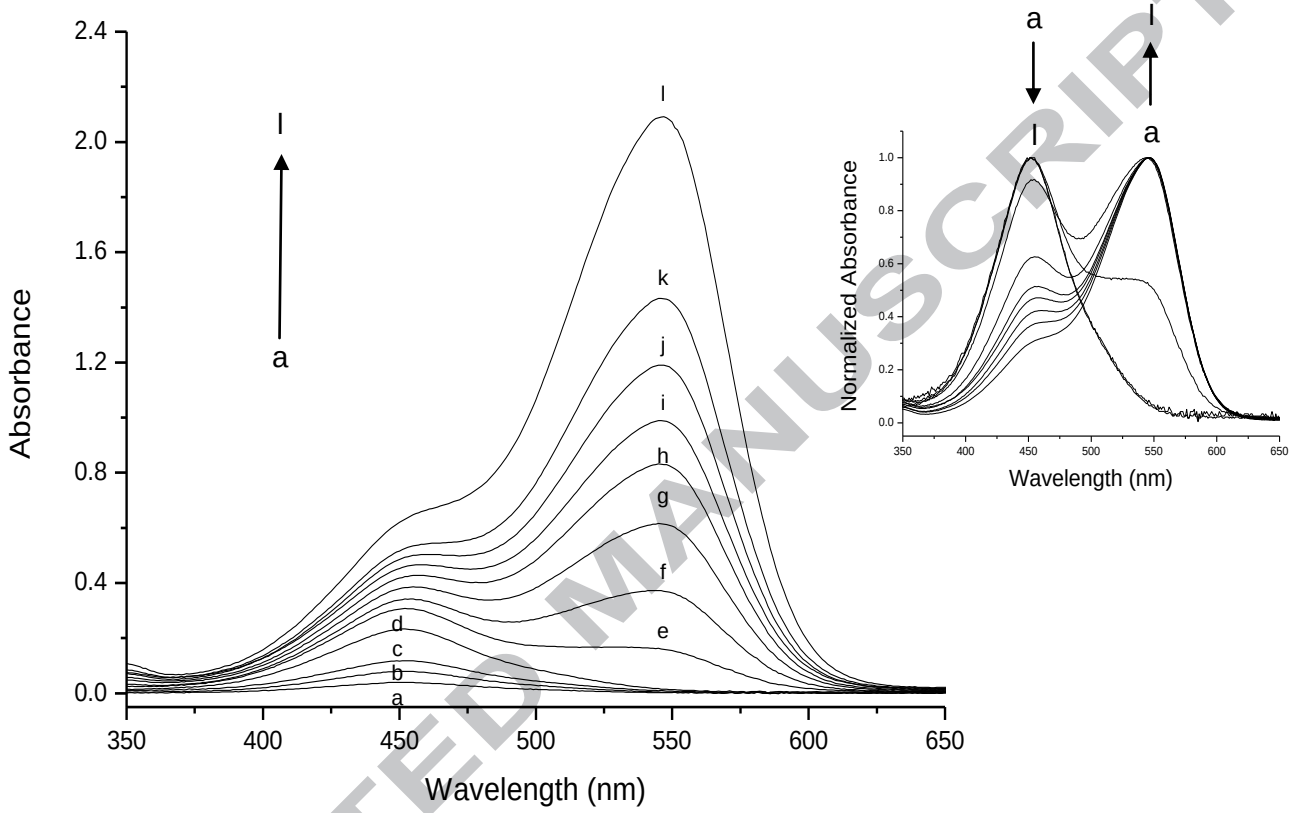

Figure Caption 4

Figure 4: Absorption spectra of **NRBr** at different concentrations in ethanol. [**NRBr**] (a) 2.71×10^{-6} M, (l) 9.49×10^{-5} M. Inset: Normalized absorption spectra at maximum absorption wavelength as a function of concentration.

Figure 5

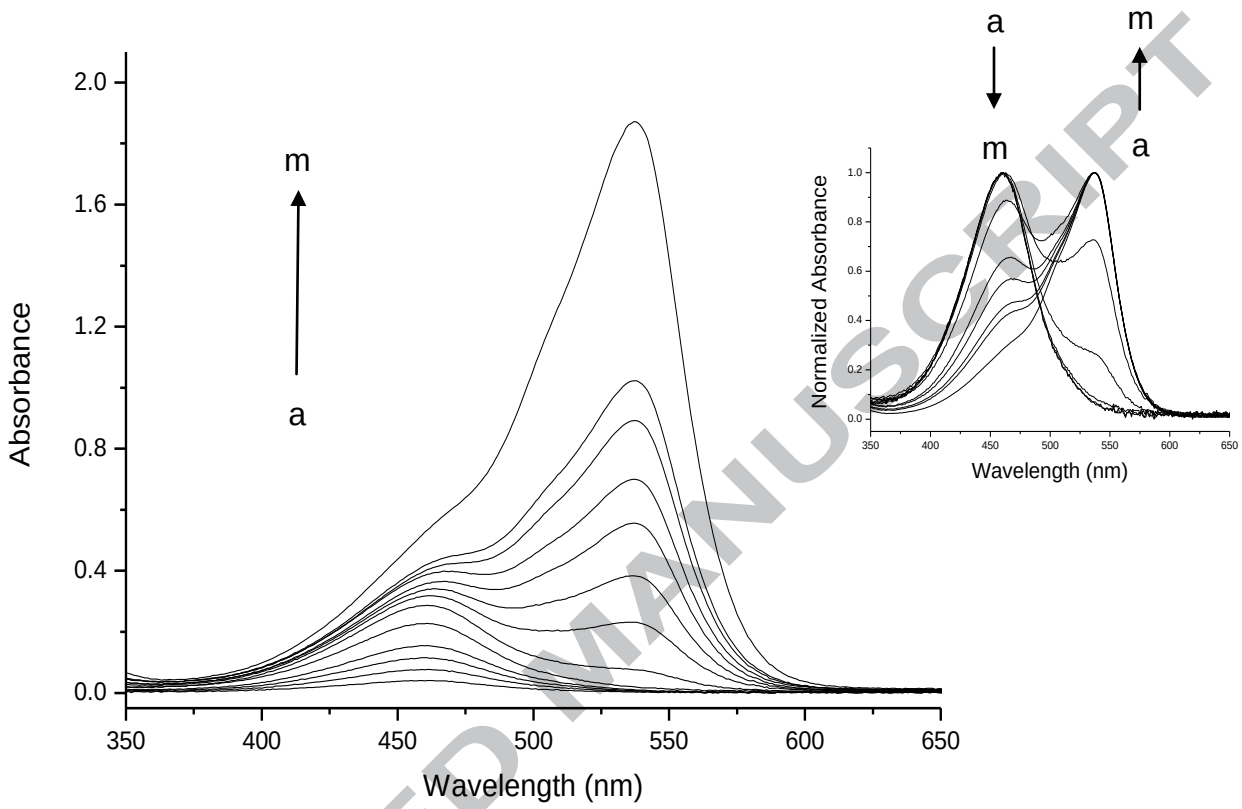

Figure Caption 5

Figure 5: Absorption spectra of **NR** at different concentrations in ethanol. [**NR**] (a) 1.73×10^{-6} M, (m) 5.19×10^{-5} M. Inset: Normalized absorption spectra at maximum absorption wavelength as a function of concentration.

Figure 6 A

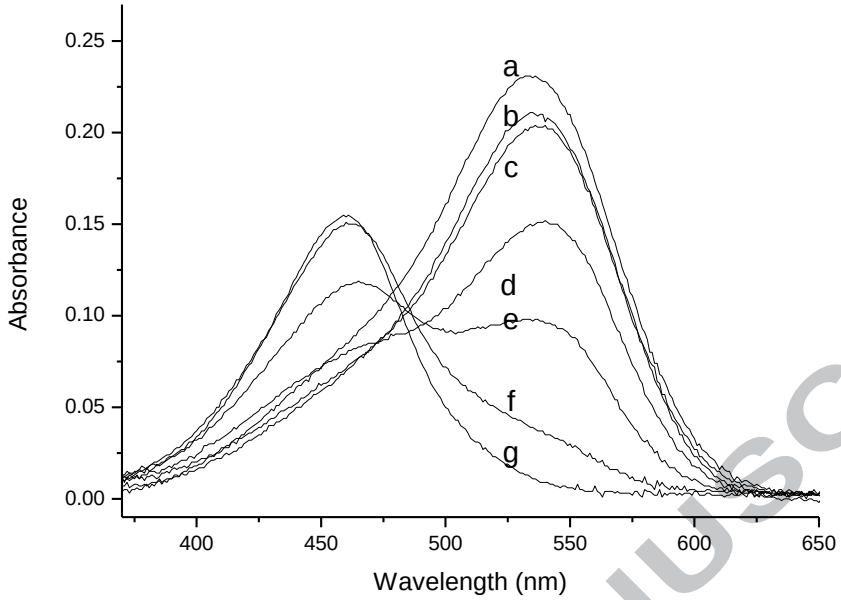

Figure Caption 6 A

Figure 6 A: Changes in UV-Vis spectra of **NR** at 6.93 x 10^{-6} M in water with an increasing amount of ethanol in the solution. Proportions water:ethanol a) 100:0; b) 95:5; c) 90:10; d) 75:25; e) 50:50; f) 25:75; g) 0:100.

Figure 6 B

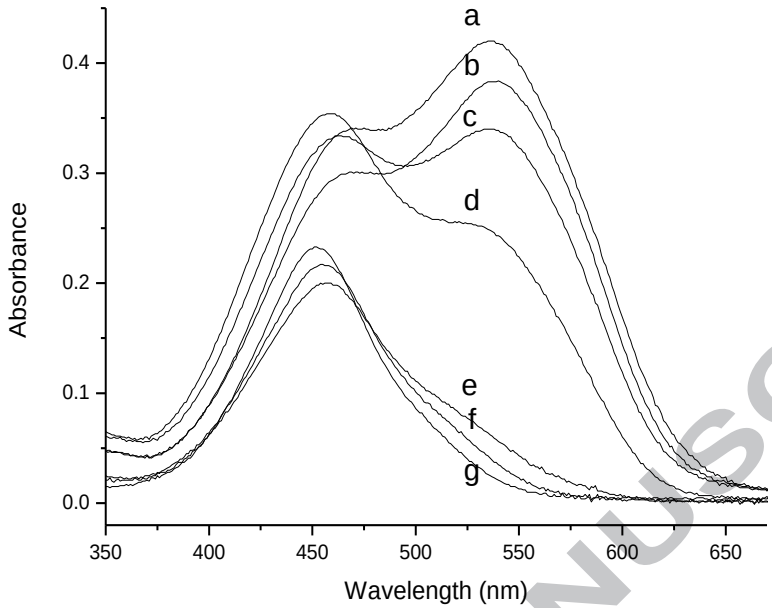

Figure Caption 6 B

Figure 6 B: Changes in UV-Vis spectra of **NRBr** at 2.71 x 10^{-5} M in water with an increasing amount of ethanol in the solution. Proportions water:ethanol a) 100:0; b) 95:5; c) 90:10; d) 75:25; e) 50:50; f) 25:75; g) 0:100.

Figure 7

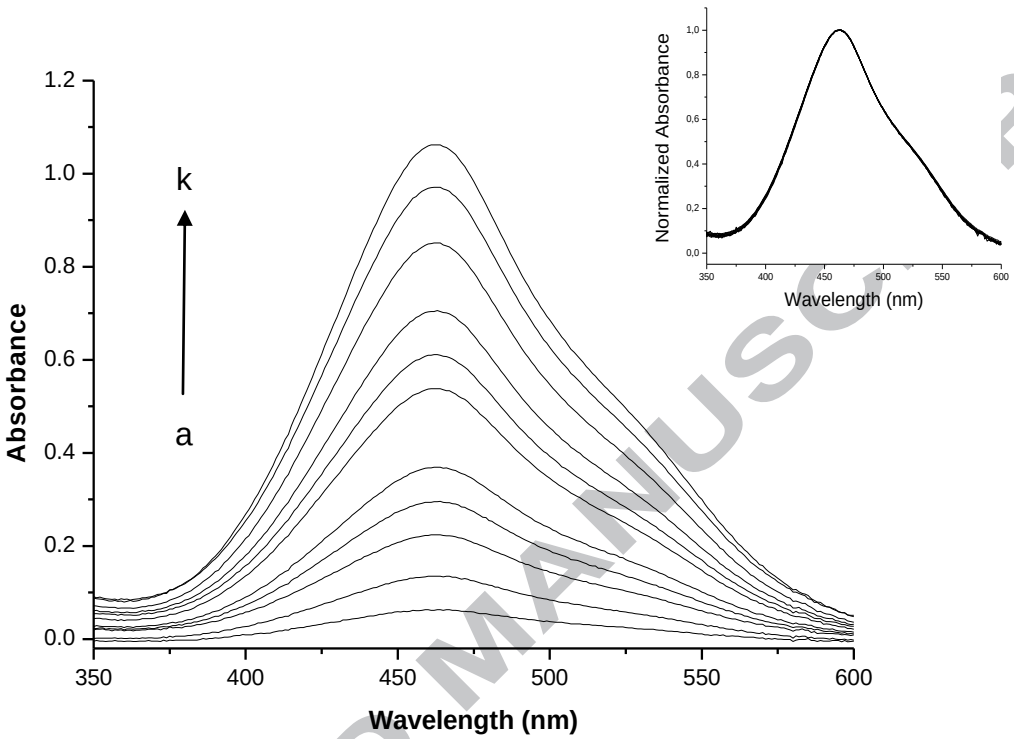

Figure Caption 7

Figure 7: Absorption spectra of **NRBr** at different concentrations in water:PEG 400 mixture 75:25 v/v. [**NRBr**] (a) 5.42×10^{-6} M, (k) 8.14×10^{-5} M. Inset: Normalized absorption spectra at maximum absorption wavelength as a function of concentration.

Figure 8

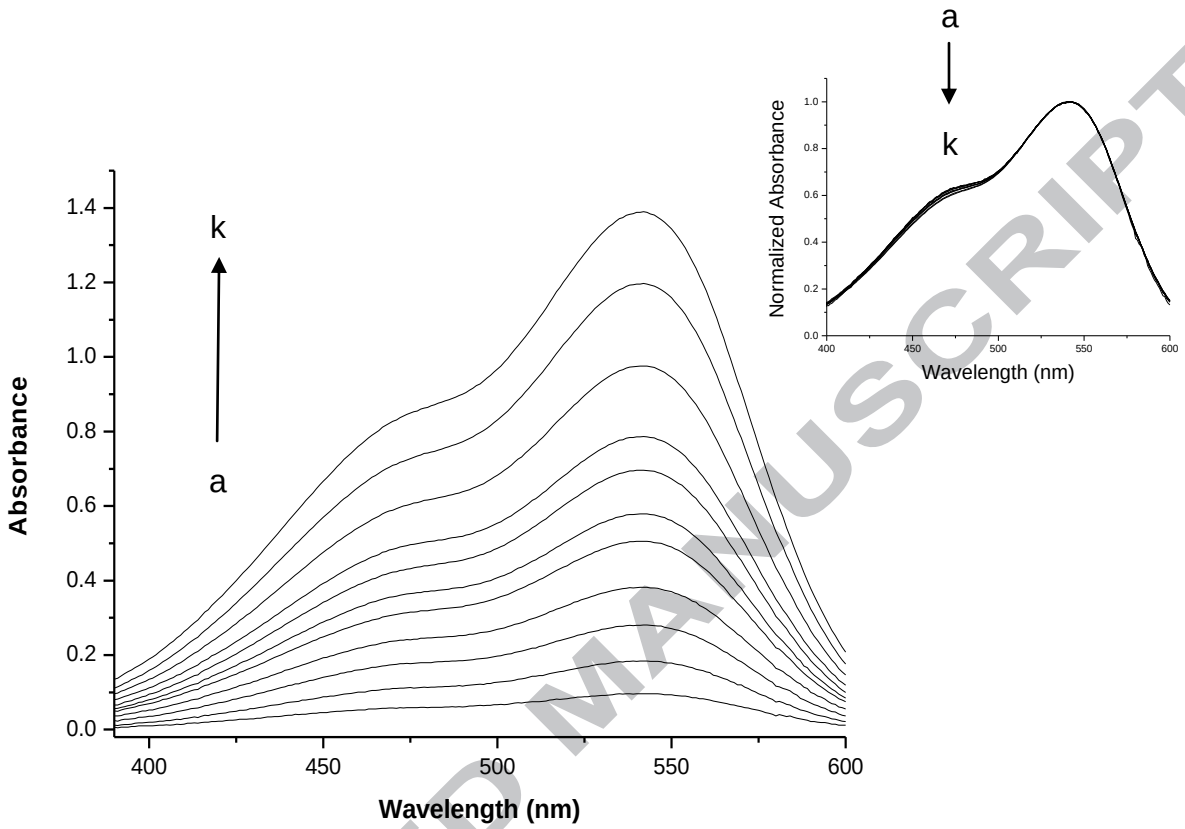

Figure Caption 8

Figure 8: Absorption spectra of **NR** at different concentrations in water:PEG 400 mixture 75:25 v/v. [**NR**] (a) 3.46×10^{-6} M, (k) 4.85×10^{-5} M. Inset: Normalized absorption spectra at maximum absorption wavelength as a function of concentration.

Figure 9 A

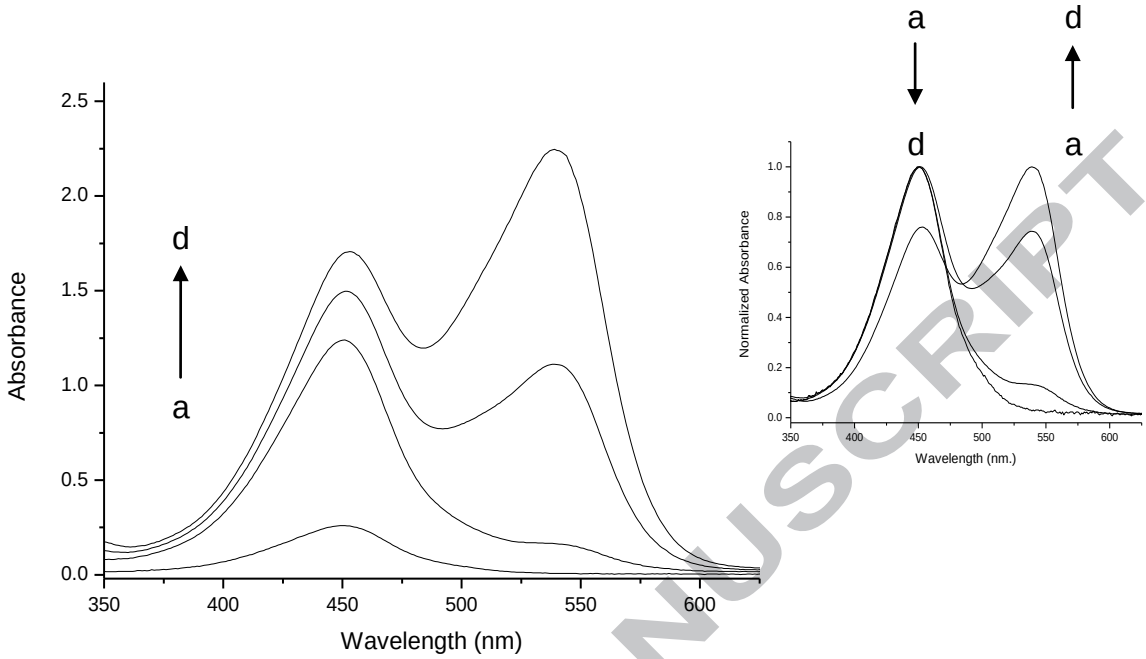

Figure Caption 9

Figure 9 A: Absorption spectra of **NR** at different concentrations in DMF. [**NR**] (a) 6.93×10^{-6} M, (d) 6.93×10^{-5} M. Inset: Normalized absorption spectra at maximum absorption wavelength as a function of concentration.

Figure 9 B

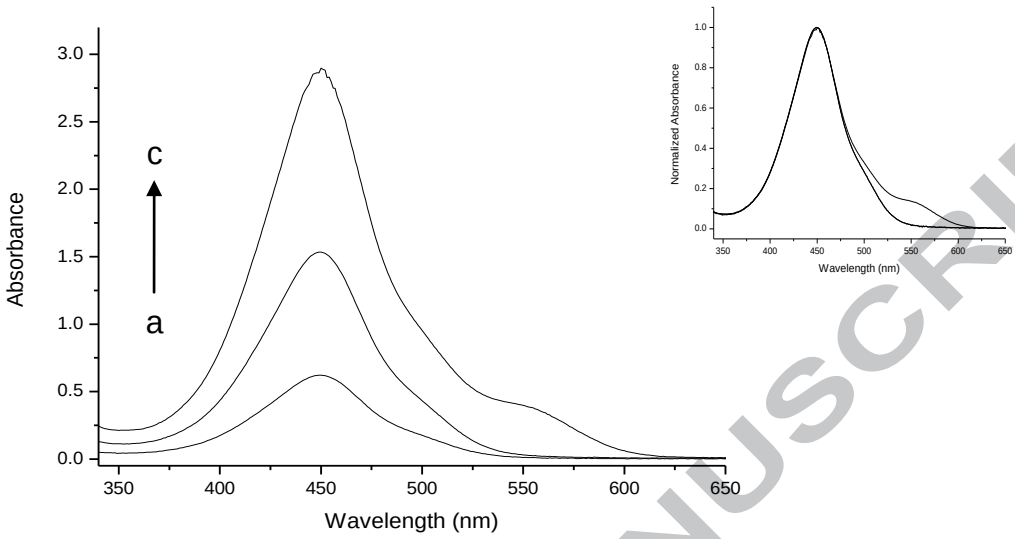

Figure Caption 9 B

Figure 9 B: Absorption spectra of **NRBr** at different concentrations in DMF. [**NRBr**] (a) 5.42×10^{-5} M, (c) 2.71×10^{-4} M. Inset: Normalized absorption spectra at maximum absorption wavelength as a function of concentration.

Figure 10 A

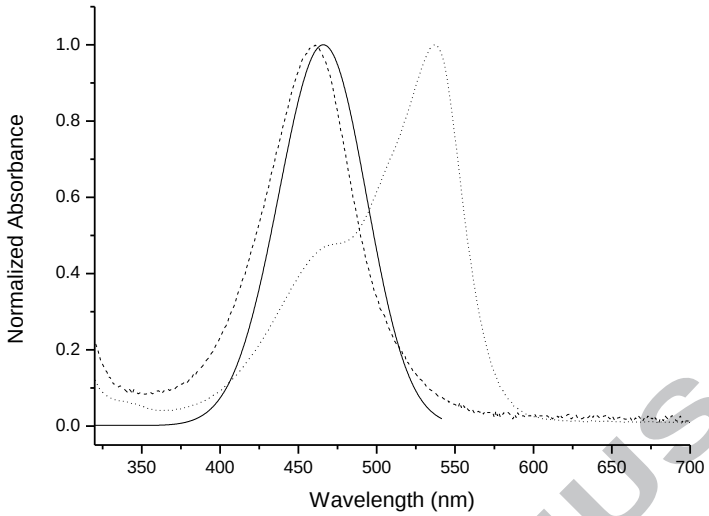

Figure Caption 10 A

Figure 10 A: Theoretical and experimental visible absorption band for **NR** in ethanol. Solid-line: Theoretical spectrum of monomer; dashed-line: Experimental spectrum of monomer; dotted-line: Experimental spectrum of aggregate.

Figure 10 B

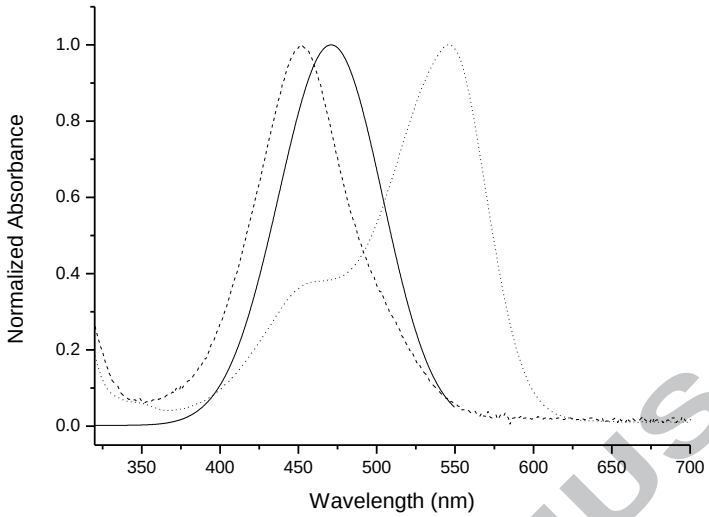

Figure Caption 10 B

Figure 10 B: Theoretical and experimental visible absorption band for **NRBr** in ethanol.Solid-line: Theoretical spectrum of monomer; dashed-line: Experimental spectrum of monomer; dotted-line: Experimental spectrum of aggregate.

Graphical Abstract

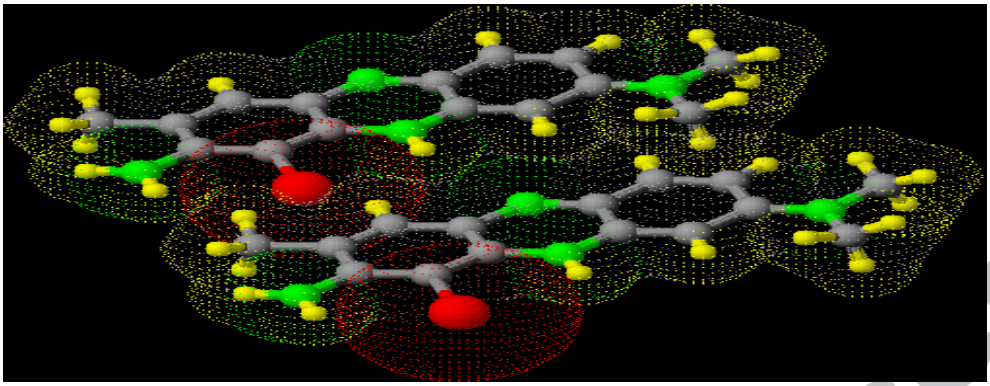

Highlights

✓ Synthesis of Neutral Red monobrominated.

✓ Aggregation of Neutral Red and Neutral Red monobrominated in different media.

✓ Theoretical calculation of the Neutral Red and Neutral Red monobrominated monomers.